nature geoscience

ARTICLES

PUBLISHED ONLINE: 28 NOVEMBER 2016 | DOI: 10.1038/NGEO2844

Constraints on ocean carbonate chemistry and p_{CO_2} in the Archaean and Palaeoproterozoic

C. L. Blättler[1]*, L. R. Kump[2], W. W. Fischer[3], G. Paris[3†], J. J. Kasbohm[1] and J. A. Higgins[1]

One of the great problems in the history of Earth's climate is how to reconcile evidence for liquid water and habitable climates on early Earth with the Faint Young Sun predicted from stellar evolution models. Possible solutions include a wide range of atmospheric and oceanic chemistries, with large uncertainties in boundary conditions for the evolution and diversification of life and the role of the global carbon cycle in maintaining habitable climates. Increased atmospheric CO_2 is a common component of many solutions, but its connection to the carbon chemistry of the ocean remains unknown. Here we present calcium isotope data spanning the period from 2.7 to 1.9 billion years ago from evaporitic sedimentary carbonates that can test this relationship. These data, from the Tumbiana Formation, the Campbellrand Platform and the Pethei Group, exhibit limited variability. Such limited variability occurs in marine environments with a high ratio of calcium to carbonate alkalinity. We are therefore able to rule out soda ocean conditions during this period of Earth history. We further interpret this and existing data to provide empirical constraints for carbonate chemistry of the ancient oceans and for the role of CO_2 in compensating for the Faint Young Sun.

The Faint Young Sun paradox[1] has numerous hypothetical solutions[2], but observational tests that can distinguish among them are rare. Increased CO_2 is a likely contributor, given its importance as a greenhouse gas today and its role in silicate–carbonate cycling over geologic timescales[3,4]; however, huge uncertainties exist in p_{CO_2} reconstructions for early Earth[5]. These uncertainties extend to the abundance of dissolved CO_2 in the oceans, including some suggestions[6,7] for the existence of a vast reservoir of dissolved carbonate species (a 'soda ocean', with $HCO_3^- > Ca^{2+}$). Such oceanic conditions could exist in equilibrium with a wide range of proposed p_{CO_2}, with different climatic implications, but require very different seawater chemistry than today with respect to pH and carbonate alkalinity ($ALK = HCO_3^- + 2 \cdot CO_3^{2-}$, hereafter referred to simply as alkalinity). Narrowing the possible p_{CO_2}–pH conditions for early Earth is therefore essential for identifying viable solutions to the Faint Young Sun paradox.

An application for stable isotopes of calcium

This study introduces an independent constraint on carbonate chemistry in the Archaean and Palaeoproterozoic using measurements of calcium isotope ratios in sedimentary carbonate precipitates. During drawdown of calcium ions, the ratio of calcium to alkalinity influences calcium isotope behaviour and creates a link to the p_{CO_2}–pH system. This approach is based on previous work[8] in marine $CaSO_4$ evaporites showing how variability in calcium isotopic composition of Phanerozoic evaporites reflects the Ca/SO_4 ratio of coeval seawater. These evaporites can distinguish high and low ratios (greater or less than 1.5 mol mol^{-1}) of calcium to sulfate in the fluid from which they precipitated, on the basis of the depletion of calcium ions and associated Rayleigh distillation of calcium isotopes (reported as $\delta^{44/40}Ca = [(^{44}Ca/^{40}Ca)_{sample}/(^{44}Ca/^{40}Ca)_{standard} - 1] \times 1{,}000$). A small $\delta^{44/40}Ca$ range indicates high Ca/SO_4, such that calcium is not substantially depleted by $CaSO_4$ salts; a large $\delta^{44/40}Ca$ range results from low Ca/SO_4, where preferential removal of lighter calcium isotopes into sulfate minerals leads to substantial positive $\delta^{44/40}Ca$ enrichments in the calcium-depleted brines and late-stage precipitates just prior to the onset of halite precipitation (Fig. 1). In this study, this relationship is generalized to other calcium-bearing minerals that express isotopic fractionation during precipitation—specifically, evaporative carbonate minerals.

Distillation of calcium isotopes during carbonate mineral precipitation can occur when alkalinity is much greater than the calcium concentration ($ALK \gg Ca$). This behaviour has been observed in Mono Lake, California ($pH = 9.8$ and $Ca/ALK = 10^{-4}$), where large temporal variability (~2.5‰) in lake water $\delta^{44/40}Ca$ was caused by changes in lake hydrology and calcium depletion[9]. Modern marine settings ($Ca/ALK = 4.1$) have insufficient alkalinity to drive such distillation, which should occur when Ca/ALK is less than 0.75, a factor of two less than the analogous Ca/SO_4 threshold because of the difference in charge equivalence. Of all the major ions in seawater, this behaviour is exclusive to calcium, whose carbonate and sulfate minerals are the first to precipitate readily from concentrating seawater and whose isotopic behaviour is largely controlled by precipitation of those minerals. By comparison with sulfate evaporites and Mono Lake, highly alkaline conditions should therefore be identifiable in the geologic record by large calcium isotope variability in environments where calcium is being locally depleted, characterized by positive enrichments in $\delta^{44/40}Ca$ over the baseline for open marine carbonates. Such environments can be found under evaporitic conditions—for example, where the sedimentary record indicates the presence of halite. The calcium isotope observations then may translate to limits on Ca/ALK in ancient settings, with implications for ancient seawater carbonate chemistry and p_{CO_2}–pH.

The calcium isotopic composition of ancient carbonates

Three geologic units were analysed to investigate calcium isotope behaviour in ancient carbonates which experienced evaporitic conditions (additional details in Supplementary Methods and

[1]Department of Geosciences, Princeton University, Princeton, New Jersey 08544, USA. [2]Department of Geosciences, Pennsylvania State University, University Park, Pennsylvania 16802, USA. [3]Division of Geological and Planetary Sciences, California Institute of Technology, Pasadena, California 91125, USA. [†]Present address: CRPG, UMR 7358, CNRS—Université de Lorraine, 54500 Vandoeuvre-lès-Nancy, France. *e-mail: blattler@princeton.edu

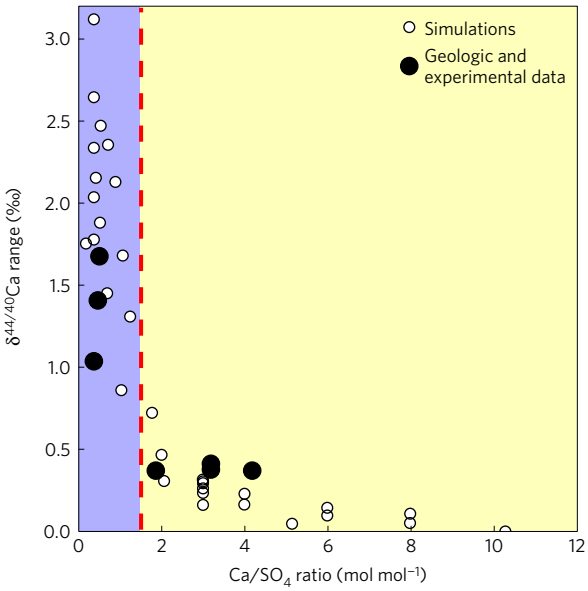

Figure 1 | Calibration of calcium isotope range to Ca/SO_4 in evaporites. Dashed line shows the threshold between large (>0.75‰) and small (<0.75‰) $\delta^{44/40}$Ca ranges. Evaporite simulations (open circles) are described in Methods. Data (filled circles) represent Phanerozoic evaporite sections[8] with Ca/SO_4 estimated from halite fluid inclusions as well as beaker evaporation experiments.

Supplementary Figs 2–6). These units were selected as the best-available candidates to express local evaporative distillation of calcium in such ancient settings. Dated at 2.7 Ga (Gyr ago; ref. 10), the Tumbiana Formation (Fortescue Group, Western Australia) includes a sequence of shallow-water carbonates and siliciclastics (tens to 100 metres thick), the Meentheena Member, which lies between basalts and volcaniclastic sediments and has been variously interpreted as a giant lacustrine system[11] or a coastal/shallow marine setting[12]. The conclusions below regarding p_{CO_2} remain valid under either interpretation, given that both depositional environments reflect shallow waters in equilibrium with the atmosphere. Dated at 2.6–2.5 Ga (ref. 13), the Campbellrand Platform (Transvaal Supergroup, South Africa) is a well-preserved carbonate ramp-to-shelf sequence containing abundant marine cements and a range of shallow- to deep-water carbonate facies[14,15]. The Pethei Group (Great Slave Lake Supergroup, Northwest Territories, Canada) is the youngest of the three units at approximately 1.9 Ga (ref. 16). It preserves both shallow- and deep-water marine facies in an alternating carbonate reef/ramp complex, and is overlain by the Stark Formation, interpreted as a halite solution-collapse breccia[17].

Limestones from the Tumbiana Formation were sampled from a single 95-m-thick section at approximately 5 m resolution. Multiple sections of the Campbellrand Platform are represented in this study, including normal marine (non-evaporitic) carbonate facies featuring exceptionally well preserved herringbone calcite cements[18], as well as two platformal sections from the Gamohaan and Frisco Formations (WJG3 and WJG9, respectively) whose isopachous cements and vuggy textures are interpreted to reflect evaporitic, lagoonal environments. Section WJG3 is predominantly limestone, whereas WJG9 is pervasively dolomitized (Mg/Ca ≈ 0.9). These sections were sampled at both 5–10 m and cm-scale resolution (that is, multiple areas within a hand sample). While direct evidence for halite was not observed in these sections of the Tumbiana and Campbellrand, halite casts are present elsewhere along strike[15,19,20] and confirm that these depositional units experienced periodic evaporitic conditions.

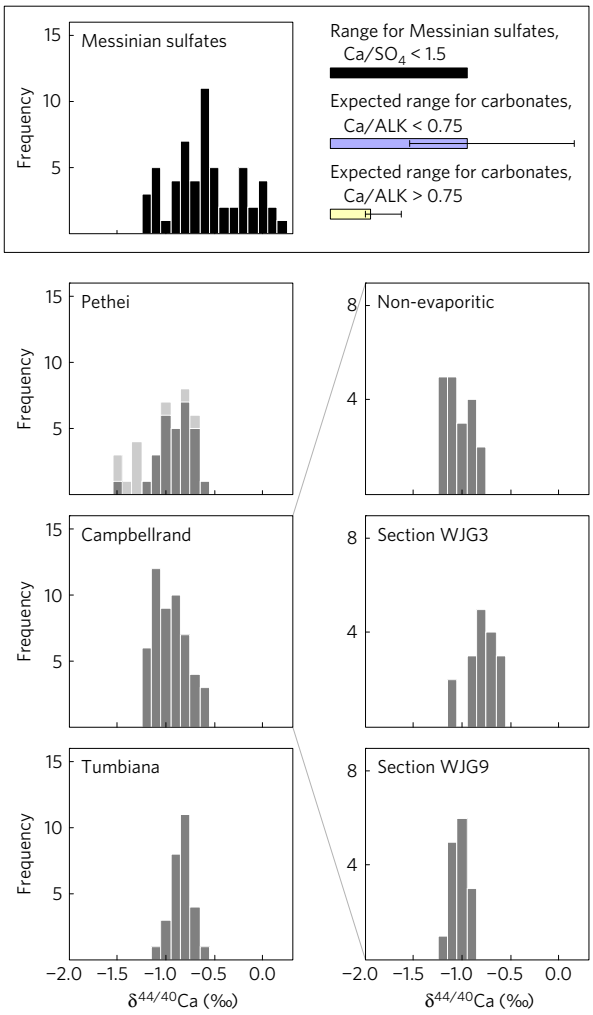

Figure 2 | Histograms of calcium isotope data from three Archaean–Palaeoproterozoic sections (grey) and Messinian sulfate data[8] from the Mediterranean (black) for comparison. Lighter-grey Pethei samples are from evaporitic sections, including the overlying collapse breccia[21]. Data from the Campbellrand are shown both as a single data set and as three separate populations: deeper water non-evaporitic carbonate facies and two evaporitic sections (WJG3 limestones and WJG9 dolomites).

Samples from the Pethei Group are partially dolomitized and represent several sections from across the platform and slope[21]. A handful of samples record the transition into the overlying breccia of the Stark Formation. Abundant halite casts and the solution-collapse origins of the Stark Formation support the interpretation of an evaporitic progression from carbonate directly to halite precipitation[7]. The documentation of halite in all three of the sampled units is essential for interpreting calcium isotope variability, which is maximally expressed during the complete evaporitic titration of calcium by available carbonate and/or sulfate ions; failure to reach halite saturation would result in a fraction of the full $\delta^{44/40}$Ca isotopic distillation being expressed.

Calcium isotope data from Tumbiana, Campbellrand, and Pethei carbonates express restricted ranges compared to Messinian-aged $CaSO_4$ minerals (Fig. 2 and Table 1 and Supplementary Table 1), suggesting, by analogy to the relationship of sulfate evaporites to Ca/SO_4, that Archaean and Proterozoic seawater had high Ca/ALK, similar to the modern ocean. The narrower distributions of the ancient carbonates become even more distinct through examination of the geologic context of the Campbellrand and Pethei samples. Con-

Table 1 | Statistics for calcium isotope data shown in Fig. 2.

Sample set	Age (Ga)	N	$\delta^{44/40}$Ca mean (‰)	$\delta^{44/40}$Ca range (‰)	σ (1 s.d.)
Messinian sulfates	0.006	58	−0.57	1.44	0.37
Pethei	1.9	39	−0.98	0.85	0.25
Non-evaporitic*		28	−0.88	0.51	0.15
Campbellrand	2.6	54	−0.96	0.86	0.17
Non-evaporitic		19	−1.04	0.36	0.13
Section WJG3		17	−0.79	0.49	0.14
Section WJG9		15	−1.02	0.23	0.07
Tumbiana	2.7	28	−0.85	0.45	0.11

*Excluding a single outlier.

sidering the three stratigraphic subsets of the Campbellrand (deeper subtidal facies, shallow-water limestones of WJG3, and shallow-water dolomites of WJG9), each of these sections is characterized by $\delta^{44/40}$Ca values that vary by less than 0.5‰, comparable to the single section of the Tumbiana (range = 0.45‰). This range is only ~35% of the 1.44‰ range observed in Messinian sulfates, deposited under low-Ca/SO_4 conditions where calcium isotopes were extensively distilled, and ~20% of the 2.5‰ variability in dissolved calcium in Mono Lake, a low-Ca/ALK system.

The Pethei data set skews towards more negative $\delta^{44/40}$Ca, although excluding the most evaporitic facies (sections 5 and 6 from Hotinski *et al.*[21]) and a single outlier, it has a similarly restricted range (0.51‰) to the other ancient carbonates. The evaporitic sections (Fig. 2, lighter grey), however, extend the measured $\delta^{44/40}$Ca down to −1.50‰. The predicted isotopic behaviour during evaporative titration of calcium by precipitation of carbonate minerals is enrichment in ^{44}Ca. The observed depletion in $\delta^{44/40}$Ca may be caused either by an increased fractionation of calcium isotopes or by diagenetic (meteoric) alteration. If a greater fractionation were the cause of the shift to more negative $\delta^{44/40}$Ca, the magnitude of calcium isotope distillation would be enhanced for a given fraction of calcium removed; therefore, the lack of positive $\delta^{44/40}$Ca in the uppermost stratigraphy remains consistent with high initial Ca/ALK. It seems more likely that these samples experienced meteoric diagenesis during the dissolution event that brecciated the Stark Formation, especially given the origins of certain samples from the collapse breccia itself. No difference in $\delta^{44/40}$Ca is observed between shallow-water and deep-water carbonate facies, suggesting that baseline carbonate $\delta^{44/40}$Ca was around −0.9‰ and that these data lack a $\delta^{44/40}$Ca enrichment (instead of the true baseline $\delta^{44/40}$Ca lying close to the minimum value recorded, −1.5‰, and the bulk of the data set reflecting isotopic enrichment of up to 1‰).

This interpretation that restricted calcium isotope ratios reflect high Ca/ALK assumes that the fractionation between carbonates and seawater has remained constant through time. While a similar fractionation (between −1.0 and −1.3‰) is observed for both modern marine settings and Mono Lake[9,22], there are no direct constraints on this variable for the Archaean–Palaeoproterozoic. However, to explain the observed distributions with low Ca/ALK would require a fractionation less than 0.25‰ between seawater and carbonate minerals, a value consistent with extremely slow rates (near-equilibrium) of precipitation[23] and not expected during non-equilibrium evaporative carbonate precipitation. Other sources of variability in carbonate $\delta^{44/40}$Ca include mineralogy[24] and rate-dependent effects[25]. However, no marine carbonates have yet been measured with 1–2‰ enrichments in $\delta^{44/40}$Ca over the bulk silicate Earth value[22], so the behaviour observed in Messinian sulfates and Mono Lake waters (but not in the ancient carbonates) appears to be uniquely diagnostic of calcium depletion through mineral precipitation.

Implications for ocean carbonate chemistry and p_{CO_2}

The limited $\delta^{44/40}$Ca variability of Archaean and Proterozoic shallow-water carbonate sediments provides an empirical constraint that Ca/ALK > 0.75 in ancient seawater. Because the equilibrium carbonate system has a unique solution only when two chemical variables (p_{CO_2}, $CO_{2(aq)}$, HCO_3^-, CO_3^{2-}, pH, ALK, or dissolved inorganic carbon) are known, this constraint defines an area in p_{CO_2}–pH space with possible solutions to the lower left of a curve of constant Ca/ALK (Fig. 3). The position of this curve is sensitive to the calcite saturation state ($\Omega = [Ca^{2+}] \times [CO_3^{2-}]/K_{sp}$), for which reasonable bounds are $\Omega = 1$, the minimum saturation state for the formation and preservation of limestone, and $\Omega = 6$, the supersaturated state of modern tropical surface waters and a generous estimate for an anoxic ocean[26]. As expected, modern surface ocean conditions exist on the left of the $\Omega = 6$ curve (high-Ca/ALK, small-$\delta^{44/40}$Ca range induced by carbonate precipitation), whereas Mono Lake conditions exist on the right side (low-Ca/ALK, large-$\delta^{44/40}$Ca range).

This threshold for calcium isotope behaviour as a function of Ca/ALK rules out a number of hypotheses about early Earth conditions. The area (shaded yellow) to the lower left of Fig. 3 denotes the region where limited calcium isotope distillation occurs, which is consistent with the ancient carbonate $\delta^{44/40}$Ca data in this study. The area (shaded blue) to the upper right indicates the region where substantial calcium isotope distillation is expected because of excess alkalinity, including the 'soda ocean hypothesis' and other preferred seawater conditions[6,7]. In ruling out these high-ALK solutions, this study also reverses the favoured explanation for the absence of sulfate minerals in evaporite sequences older than 1.6 Ga (ref. 7). Rather than suppressing gypsum precipitation by depleting calcium through carbonate mineral precipitation (which would induce isotopic enrichment), low sulfate concentrations were probably responsible for the lack of gypsum in older evaporite sequences.

The constraint that seawater Ca/ALK > 0.75 during at least three intervals from 2.7 to 1.9 Ga provides a way of differentiating between the contributions of CO_2 and other greenhouse gases towards any solution to the Faint Young Sun paradox. Noting that neither proxy estimates of CO_2[5] nor three-dimensional climate model calculations[27,28] have reached a consensus on required ancient atmospheric compositions, Fig. 3 explores the implications of a palaeosol-based CO_2 estimate[29] and a climate model result[27] at one particular age (2.5 Ga). A lower range of seawater pH is predicted under higher-CO_2 conditions, which are consistent with some models, compared to the solution space compatible with one interpretation of palaeosol proxy results[29], which may require additional sources of radiative forcing. The difference in pH is substantial: ~0.3 pH units for a $\log(p_{CO_2})$ difference of 0.5. Any robust limits on seawater pH would therefore be a strong constraint on viable concentrations of CO_2 on early Earth.

In addition to the trade-off between seawater pH and atmospheric p_{CO_2}, this study generates a number of other predictions for ancient seawater chemistry under high- or low-CO_2 conditions. Seawater calcium concentrations are generally expected to be higher than today, particularly under higher-CO_2 conditions (Fig. 3 and Supplementary Fig. 1). These results also limit the size of the dissolved inorganic carbon (DIC) reservoir, with a likely range between 5 and 30 mmol kg^{-1}, and with the higher values again associated with higher-CO_2 conditions. The concentrations of these species directly influence the buffering capacity of seawater to local changes in DIC and ALK; with higher DIC increasing both the response time of the global carbon cycle to external perturbations and the magnitude of the carbon source/sink required to cause measurable global perturbations. These differences may explain, in part, the general stability of marine carbonate δ^{13}C values early in Earth history[30].

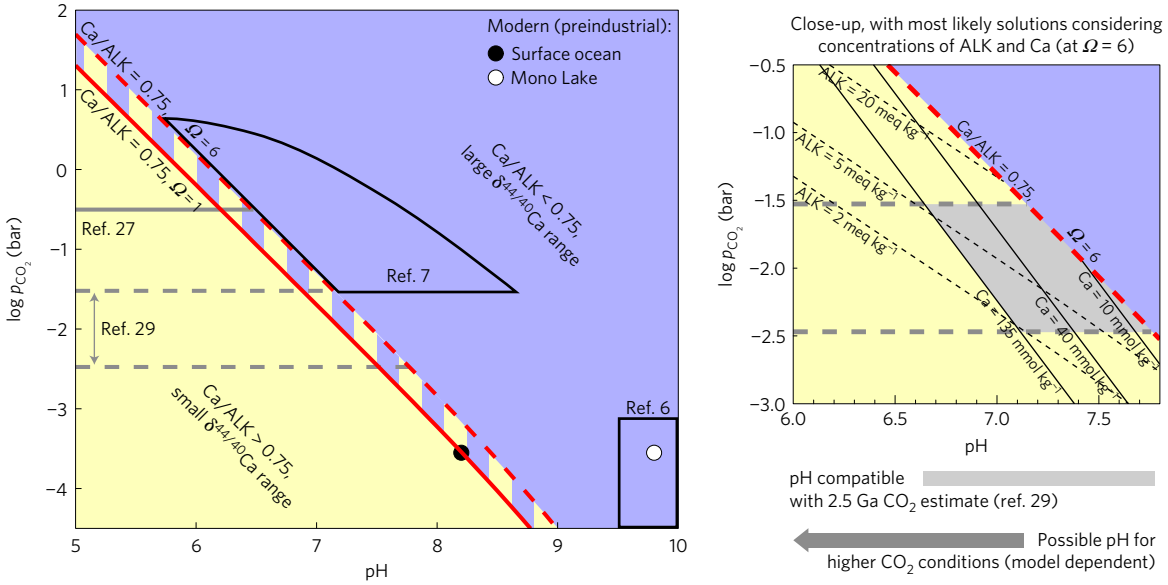

Figure 3 | Equilibrium carbonate chemistry solutions in p_{CO_2}–pH space, divided by the calcium isotope constraint that Ca/ALK > 0.75. Permissible solutions are shown in yellow; the blue region is inconsistent with data from this study. Uncertainty in the boundary between these regions from assuming different calcite saturation states is reflected in the striped zone between the solutions for Ca/ALK = 0.75 at $\Omega = 1$ and $\Omega = 6$. Black outlines indicate preferred solution spaces from previous work. Grey horizontal lines show various estimates for p_{CO_2}: solid line is a model result[27] for obtaining a mean surface temperature of 288 K (compatible with a mostly ice-free Archaean) at 2.5 Ga with increased CO_2 alone; dashed grey lines reflect upper and lower limits on p_{CO_2} estimated from a 2.5-Ga palaeosol[29]. The close-up view shows contours of ALK and Ca concentration at $\Omega = 6$, with a reasonable upper limit on Ca (see Supplemental Methods) used to further define the likely solution space.

The calcium isotope data presented here from ancient evaporitic carbonate sequences provide a valuable empirical constraint on ancient oceanic and atmospheric composition that permits a direct test of solutions to the Faint Young Sun paradox if seawater pH or calcium concentrations can be determined independently. As a major constituent of carbonate rocks, calcium isotopes carry high preservation potential and a unique relationship to the carbon cycle. To be consistent with the $\delta^{44/40}Ca$ data for the time intervals represented by these sedimentary rocks, which occur both before and after the Great Oxidation Event, solutions for offsetting the Faint Young Sun must balance p_{CO_2} and pH. High-p_{CO_2} atmospheres are possible as long as oceanic pH is low and calcium concentrations are high; high-alkalinity soda oceans are not. Further predictions for pH, calcium, and DIC open up new ways to test hypotheses about early Earth environments and the role of CO_2 in maintaining habitable climates.

Methods

Methods, including statements of data availability and any associated accession codes and references, are available in the online version of this paper.

Received 7 June 2016; accepted 25 October 2016; published online 28 November 2016

References

1. Sagan, C. & Mullen, G. Earth and Mars: evolution of atmospheres and surface temperatures. *Science* **177,** 52–56 (1972).
2. Feulner, G. The Faint Young Sun problem. *Rev. Geophys.* **50,** RG2006 (2012).
3. Walker, J. C. G., Hays, P. B. & Kasting, J. F. A negative feedback mechanism for the long-term stabilization of the Earth's surface temperature. *J. Geophys. Res.* **86,** 9776–9782 (1981).
4. Berner, R. A., Lasaga, A. C. & Garrels, R. M. The carbonate–silicate geochemical cycle and its effect on atmospheric carbon dioxide over the past 100 million years. *Am. J. Sci.* **283,** 641–683 (1983).
5. Kasting, J. F. Early Earth: Faint Young Sun redux. *Nature* **464,** 687–689 (2010).
6. Kempe, S. & Degens, E. T. An early soda ocean? *Chem. Geol.* **53,** 95–108 (1985).
7. Grotzinger, J. P. & Kasting, J. F. New constraints on Precambrian ocean composition. *J. Geol.* **101,** 235–243 (1993).
8. Blättler, C. L. & Higgins, J. A. Calcium isotopes in evaporites record variations in Phanerozoic seawater SO_4 and Ca. *Geology* **42,** 711–714 (2014).
9. Nielsen, L. C. & DePaolo, D. J. Ca isotope fractionation in a high-alkalinity lake system: Mono Lake, California. *Geochim. Cosmochim. Acta* **118,** 276–294 (2013).
10. Blake, T., Buick, R., Brown, S. & Barley, M. Geochronology of a Late Archaean flood basalt province in the Pilbara Craton, Australia: constraints on basin evolution, volcanic and sedimentary accumulation, and continental drift rates. *Precambrian Res.* **133,** 143–173 (2004).
11. Awramik, S. M. & Buchheim, H. P. A giant, Late Archean lake system: the Meentheena Member (Tumbiana Formation; Fortescue Group), Western Australia. *Precambrian Res.* **174,** 215–240 (2009).
12. Sakurai, R., Ito, M., Ueno, Y., Kitajima, K. & Maruyama, S. Facies architecture and sequence-stratigraphic features of the Tumbiana Formation in the Pilbara Craton, northwestern Australia: implications for depositional environments of oxygenic stromatolites during the Late Archean. *Precambrian Res.* **138,** 255–273 (2005).
13. Sumner, D. Y. & Bowring, S. A. U–Pb geochronologic constraints on deposition of the Campbellrand Subgroup, Transvaal Supergroup, South Africa. *Precambrian Res.* **79,** 25–35 (1996).
14. Beukes, N. J. Facies relations, depositional environments and diagenesis in a major early Proterozoic stromatolitic carbonate platform to basinal sequence, Campbellrand Subgroup, Transvaal Supergroup, southern Africa. *Sediment. Geol.* **54,** 1–46 (1987).
15. Sumner, D. Y. & Grotzinger, J. P. Implications for Neoarchaean ocean chemistry from primary carbonate mineralogy of the Campbellrand–Malmani Platform, South Africa. *Sedimentology* **51,** 1273–1299 (2004).
16. Hoffman, P. in *Reefs, Canada and Adjacent Area* (eds James, N. P., Geldsetzer, H. H. J. & Tebbull, G. E.) 38–48 (Canadian Society of Petroleum Geologists Memoir 13, 1989).
17. Hoffman, P., Bell, I., Hildebrand, R. & Thorstad, L. Geology of the Athapuscow aulacogen, east arm of Great Slave Lake, District of Mackenzie. *Geol. Surv. Can. Pap.* **77-1A,** 117–129 (1977).
18. Sumner, D. Y. & Grotzinger, J. P. Herringbone calcite: petrography and environmental significance. *J. Sediment. Res.* **66,** 419–429 (1996).
19. Buick, R. The antiquity of oxygenic photosynthesis: evidence from stromatolites in sulphate-deficient Archaean lakes. *Science* **255,** 74–77 (1992).
20. Eriksson, K., Simpson, E., Master, S. & Henry, G. Neoarchaean (c. 2.58 Ga) halite casts: implications for palaeoceanic chemistry. *J. Geol. Soc.* **162,** 789–799 (2005).

21. Hotinski, R., Kump, L. & Arthur, M. The effectiveness of the Paleoproterozoic biological pump: a $\delta^{13}C$ gradient from platform carbonates of the Pethei Group (Great Slave Lake Supergroup, NWT). *Geol. Soc. Am. Bull.* **116,** 539–554 (2004).
22. Fantle, M. S. & Tipper, E. T. Calcium isotopes in the global biogeochemical Ca cycle: implications for development of a Ca isotope proxy. *Earth Sci. Rev.* **129,** 148–177 (2014).
23. Fantle, M. S. & DePaolo, D. J. Ca isotopes in carbonate sediment and pore fluid from ODP Site 807A: the Ca^{2+}(aq)–calcite equilibrium fractionation factor and calcite recrystallization rates in Pleistocene sediments. *Geochim. Cosmochim. Acta* **71,** 2524–2546 (2007).
24. Blättler, C. L., Henderson, G. M. & Jenkyns, H. C. Explaining the Phanerozoic Ca isotope history of seawater. *Geology* **40,** 843–846 (2012).
25. DePaolo, D. J. Surface kinetic model for isotopic and trace element fractionation during precipitation of calcite from aqueous solutions. *Geochim. Cosmochim. Acta* **75,** 1039–1056 (2011).
26. Higgins, J. A., Fischer, W. W. & Schrag, D. P. Oxygenation of the ocean and sediments: consequences for the seafloor carbonate factory. *Earth Planet. Sci. Lett.* **284,** 25–33 (2009).
27. Kienert, H., Feulner, G. & Petoukhov, V. Faint Young Sun problem more severe due to ice-albedo feedback and higher rotation rate of the early Earth. *Geophys. Res. Lett.* **39,** L23710 (2012).
28. Charnay, B. *et al*. Exploring the Faint Young Sun problem and the possible climates of the Archean Earth with a 3-D GCM. *J. Geophys. Res.* **118,** 10414–10431 (2013).
29. Sheldon, N. D. Precambrian paleosols and atmospheric CO_2 levels. *Precambrian Res.* **147,** 148–155 (2006).
30. Shields, G. & Veizer, J. Precambrian marine carbonate isotope database: version 1.1. *Geochem. Geophys. Geosyst.* **3,** 1–12 (2002).

Acknowledgements

This work was supported by a grant from the Simons Foundation (SCOL 339006 to C.L.B.). S. A. Maclennan and A. M. Campion aided J.J.K. in collecting Tumbiana samples. D. P. Santiago Ramos and E. A. Lundstrom contributed to laboratory analyses.

Author contributions

C.L.B. conceived of the study; L.R.K., W.W.F., G.P. and J.J.K. conducted field work and collected samples; C.L.B. and J.A.H. obtained and analysed the data.

Additional information

Supplementary information is available in the online version of the paper. Reprints and permissions information is available online at www.nature.com/reprints. Correspondence and requests for materials should be addressed to C.L.B.

Competing financial interests

The authors declare no competing financial interests.

Methods

Sample preparation and analysis. Sedimentary facies were studied in the field, followed by textural studies revealed in polished section and thin section using light microscopy. Powders were then drilled from the cut and polished surfaces, and carbonate minerals were dissolved by ultra-sonicating 5 mg of powder in a 0.1 M buffered acetic acid–ammonium hydroxide solution for up to four hours. After centrifugation and removal of the supernatant into a clean vial, separation of calcium ions was performed using a Dionex ICS-5000+ automated ion chromatography system with a fraction collector for sample recovery[31].

Calcium isotope measurements were performed on a Thermo Neptune Plus multi-collector inductively coupled plasma mass spectrometer (MC-ICP-MS) at Princeton University with an ESI Apex-IR sample introduction system, following published protocols[31]. Medium resolution slits were used to resolve isobaric interferences at masses 42 and 44, yielding an average beam size on ^{44}Ca of 4 V for a 2 ppm Ca solution. Standard-sample-standard bracketing was used to calculate $\delta^{44/42}$Ca and ensure mass-dependent fractionation among ^{44}Ca, ^{43}Ca, and ^{42}Ca. These values were converted to $\delta^{44/40}$Ca using an exponential mass law for kinetic fractionation[32], assuming $\varepsilon_{40} = 0$ (that is, no radiogenic ^{40}Ca excess). Reported values are given as $\delta^{44/40}$Ca relative to modern seawater, normalized to seawater samples analysed in the same batch as the samples, and using the carbonate standard SRM 915b to confirm accuracy. Instrumental precision, using a pure calcium standard solution measured against itself, is ±0.13‰. External reproducibility, reflecting long-term repeated analyses of standard SRM 915b processed through the chemical separation procedure as a sample, is ±0.18‰ (2σ for $\delta^{44/40}$Ca). Analyses at Princeton of SRM 915b ($\delta^{44/40}$Ca = −1.16‰, $n = 92$) are statistically indistinguishable from reported values of −1.16 ± 0.08‰ (given SRM 915b = +0.72 ± 0.04‰ relative to SRM 915a (ref. 33), and SRM915a = −1.88 ± 0.04‰ relative to seawater[34]) and −1.13 ± 0.04‰ (ref. 35).

Simulations to support the $\delta^{44/40}$Ca to Ca/SO_4 relationship (Fig. 1) are from the EQL/EVP program[36], which tracks the chemistry of the fluid and mineral products during evaporation of seawater-like solutions through halite saturation. A constant $\delta^{44/40}$Ca fractionation of −0.95‰ (ref. 37) was used to predict the $\delta^{44/40}$Ca range over the entire precipitation sequence, assuming a Rayleigh distillation mechanism during sulfate mineral precipitation. The spread in simulation results reflects changes up to a factor of five in the gypsum to halite saturation ratio to account for uncertainties in past salinity.

Analysis of uncertainty. Calculations to determine a limit on palaeoseawater Ca/ALK have been treated as conservatively as possible to obtain a robust geochemical constraint for the Archaean and Palaeoproterozoic. The minimum Ca/ALK threshold was chosen that would be consistent with the calcium isotope data. Bounds on Ω of 1 and 6 (as described in the main text) are conservative minimum and maximum estimates, giving the maximum possible area of uncertainty in p_{CO_2}–pH space.

The equilibrium carbonate chemistry system was solved using constants from Zeebe and Wolf-Gladrow[38], which incorporate activity coefficients for aqueous species in modern seawater. The major ion composition of ancient seawater is unknown, and its effects on activity coefficients for calcium and carbonate species therefore cannot be accurately assessed. Implicit in these calculations is also the assumption that carbonate alkalinity was a good approximation for total alkalinity (as it is today).

The theoretical model of Rayleigh distillation by evaporative precipitation predicts that the range of $\delta^{44/40}$Ca depends only on the magnitude of isotopic fractionation and the fraction of calcium removed from the batch of seawater. The isotopic fractionation factor is assumed to be similar to modern fractionations observed in the oceans and Mono Lake, although variables such as temperature, salinity, and precipitation rate are unconstrained in ancient depositional environments. The Phanerozoic evaporite examples[8] suggest that these factors should not obscure the diagnostic signal of isotopic Rayleigh distillation; the Messinian evaporites, for example, reflect similar evaporitic conditions and precipitation rates to those probably experienced in other halite-bearing sediments, and reliably express the expected behaviour. The fraction of calcium removed in the ancient carbonate sequences (upon reaching halite saturation) is also assessed by analogy with the calcium sulfate system. Calcium removal in calcium sulfate minerals was calculated with the EQL/EVP program[36] with a range of initial solution chemistries. The threshold Ca/SO_4 value (1.5) used to distinguish large and small variability in $\delta^{44/40}$Ca is robust in simulations with widely varying Na, Cl, SO_4, and Ca concentrations, even across order-of-magnitude changes in the initial ratio of gypsum saturation to halite saturation relative to modern seawater. Given the lower solubility of calcium carbonate relative to calcium sulfate minerals (and the factor of two difference in charge equivalence for stoichiometric precipitation with sulfate or carbonate alkalinity), the threshold Ca/ALK = 0.75 is again a minimum estimate for explaining the observed $\delta^{44/40}$Ca behaviour, and gives the maximum possible area for consideration in p_{CO_2}–pH space.

The scale of variation in other aqueous species across the solution space is demonstrated in Supplementary Fig. 1, where contours of calcium concentration are plotted for the appropriate Ca/ALK constraint at $\Omega = 1$ and $\Omega = 6$ (upper plots) and contours of alkalinity and dissolved inorganic carbon (DIC) are also shown (lower plots, note the opposite direction of increasing values). The contours show the order-of-magnitude scale of the plot, and emphasize that regions of the plotted p_{CO_2}–pH space (for example, the lower-left corner) are unlikely as a result of unreasonably high concentrations of these species. The more realistic solution space is constrained to a narrower region bounded by the Ca/ALK constraint (in red) on the upper right and a reasonable upper limit on calcium to the lower left. Figure 3 uses a very generous upper limit on calcium of 135 mmol kg^{-1}, which is over an order of magnitude greater than modern seawater calcium, and represents complete charge balance of modern chloride concentrations with calcium and magnesium alone (that is, with negligible contributions from sodium and potassium) at Mg/Ca = 1.

Diagenesis and alteration. Samples were selected with the intention of finding the best-preserved localities and phases for calcium isotope analysis. The stoichiometry of limestones and dolomites, 40% and 22% calcium by mass, respectively, imparts a high likelihood that $\delta^{44/40}$Ca is rock-buffered and resistant to extensive alteration following lithification, although diagenetic effects that generally increase $\delta^{44/40}$Ca are possible[39]. All three geologic units reflect sub-greenschist grade metamorphism[13,17,19]. With respect to bulk geochemistry, all localities preserve δ^{13}C values that are within a few permil (‰) of 0 relative to Vienna Pee Dee Belemnite (see Supplementary Table 1), which is consistent with the long-term stability of the carbonate δ^{13}C record[30]. Additionally, excellent textural preservation in the Campbellrand (see below), including abundant herringbone calcites and aragonite fans[15,18], and preservation of a δ^{13}C gradient in the Pethei[21] suggest good potential for bulk geochemical preservation.

Geologic context and sample descriptions. *Tumbiana.* The Tumbiana Formation, corresponding to Package 7 in the sequence stratigraphic classification of Blake[40], comprises the basal Mingah Member volcaniclastic sequence overlain by the Meentheena Member carbonates and stromatolites. Samples described in this study were collected from the type section at Pelican Pool (approximately 21.32° S and 120.40° E, Supplementary Fig. 2), at which these distinct members of the Tumbiana were first described[41]. Stratigraphic observations were made at decimetre scale, and samples for stable-isotope geochemistry were collected every 50 cm where outcrop permitted, a subset of which were analysed for $\delta^{44/40}$Ca.

The Meentheena Member is offset by intervals of cover from subaerial basalt flows both above and below the measured section. At this locality, outcrop began with spheroidally weathering calcareous sandstone, which became cross-bedded with a north-to-south flow direction at the metre scale up-section. The sandstone was overlain by carbonate with laminated or ripple bedding. Climbing ripples and minor interbedded silt layers were observed in the carbonate. Stromatolites ranging from centimetre to metre scale were found throughout the section in varying degrees of abundance (isolated or mats), and were observed with both columnar and domal morphologies. A layer of well sorted millimetre-scale lapilli was found near the top of the carbonate succession in both sections. Representative photographs from the field are shown in Supplementary Fig. 3.

There are conflicting interpretations of the Tumbiana Formation as an ancient lake system[11,19,42] or as a shallow marine/coastal environment[12,43]. Both Awramik and Buchheim[11] and Sakurai *et al.*[12] concede that there are no unequivocal arguments on either side, although data exist that could be consistent with their preferred interpretations. Lateral variability in depositional environment may also be a factor in these different interpretations. While both environments would permit calcium isotope ratios in carbonates to carry information about p_{CO_2} (as they both reflect shallow-water settings in communication with the atmosphere), implications for seawater composition would of course be valid only if the Tumbiana was deposited in a marine environment.

Campbellrand. The Campbellrand–Malmani Platform in South Africa is an intensively studied Neoarchaean carbonate platform with substantial *in situ*, benthic carbonate precipitation and elaborate microbialite fabrics[14,15,44,45]. The platform is part of the Neoarchaean to early Palaeoproterozoic Transvaal Supergroup, preserved in two distinct structural basins, Griqualand West and Transvaal (Supplementary Fig. 4), and began as a carbonate ramp (now preserved as the Schmidtsdrift Subgroup) before developing into a mature, rimmed carbonate shelf spreading across the entire Kaapvaal Craton[45]. The carbonate platform drowned during a major transgression, reflected in the deposition of iron formation units of the Asbestos Hills Subgroup across the craton, the Kuruman Iron Formation in Griqualand West and the Penge Iron Formation in the Transvaal. Compared to most rocks of this age, the Campbellrand is strikingly well preserved. It remains flat-lying across Griqualand West, where metamorphism was limited to sub-greenschist facies equivalent[13]. Steep structural dips (and higher metamorphic temperatures) occur around the Bushveld Igneous Complex in the Transvaal, and acute folding and faulting appear along the western edge of the craton, where Proterozoic red beds of the Olifantshoek Group are thrust over Campbellrand rocks[14].

The calcium isotope data in this study come from five stratigraphic sections (see Supplementary Fig. 5) through the Lower Nauga/Reivilo Formation (W1 and GKP01) and the Gamohaan/Frisco Formation (WJG3, W2, and WJG9). Section W1 captures shallow subtidal palaeo-environments of the Reivilo Formation at Boetsap[15,46] during the early development of the Campbellrand platform. Textures consist of minor grainstones and abundant precipitated stromatolites, including seafloor aragonite fans. Most of the carbonates in this part of the platform have been altered with a fabric-retentive dolomitization, although some horizons in this section remain limestone. Samples from GKP01, a drill core through proximal slope facies of the Campbellrand platform collected with the Agouron Institute South African Drilling Project[44], targeted herringbone calcite associated with the deep subtidal fenestral microbialites of the Lower Nauga Formation.

Sections WJG3 and W2, sampling the Gamohaan Formation, are located at Kuruman Kop and capture the terminal drowning of the carbonate platform from a shallow lagoonal evaporitic environment (WJG3) to a subtidal microbialite facies that includes abundant early marine cements (W2)[18,45]. The lagoonal facies comprise interbedded fenestrate microbial laminations and isopachously domed limestone[45]. In the Transvaal area at the Rotterdam Farm outcrop, section WJG9 captures the Frisco Formation, laterally equivalent to the Gamohaan Formation, but deposited in a more proximal setting and with more siliciclastic-rich beds. The Frisco Formation evolved from a shallow depositional environment, as indicated by ooids (now silicified), ripple marks, and cross-laminations, to a deeper environment, eventually overlain by deposition of the Penge Iron Formation. Sections WJG3 and WJG9 were deposited in the final stage of the platform prior to its drowning (2.52 Ga), and are considered to be the most evaporitic environments sampled in the Campbellrand. Carbon and oxygen stable isotope are from Paris and colleagues[47].

Pethei. The Pethei Group represents the clearest example of an evaporitic carbonate sequence where calcium isotope distillation might have been observed. This carbonate platform/ramp to basin system is exposed on the east arm of the Great Slave Lake in the Northwest Territories, Canada, overlying the deep-water siliciclastic Kahochella Group[17]. The Taltheilei, Utsingi, Wildbread, and Hearne Formations are platformal/reefal units that transition to marginal slope facies, and eventually the basinal McLean, Blanchet, and Pekanatui Point Formations (Supplementary Fig. 6). A diversity of microbialite facies characterize peritidal, lagoonal, shelf margin, and subtidal environments[48] with directly precipitated carbonate as a major sedimentary component[16,49]. The overlying Stark Formation megabreccia, interpreted to have a solution-collapse origin[17], suggests that the environment became restricted and evaporitic in the uppermost Pethei. Deposition and later dissolution of a massive halite unit appears to have occurred directly following carbonate precipitation, and without substantial sulfate mineral precipitation[7].

Samples for calcium isotope analysis originate from a variety of environments along the ancient platform to slope to basin. Sections 1 through 6, as documented in Hotinski *et al.*[21], are all represented in this study, with additional context and information (sample names, descriptions, carbon and oxygen stable-isotope ratios, and trace element data) taken from Hotinski[50]. Samples span the range of environments from throughout the development of the Pethei Group, with the distributions of $\delta^{44/40}$Ca data across these different facies shown in Supplementary Fig. 6. No difference in the means from deep-water to platformal sections is observed, supporting the conclusion that Ca/ALK was too high to permit an isotopic enrichment during the evaporative transition to the overlying Stark Formation.

Data availability. The authors declare that the data supporting the findings of this study are available within the article and its Supplementary Information files.

References

31. Blättler, C. L., Miller, N. R. & Higgins, J. A. Mg and Ca isotope signatures of authigenic dolomite in siliceous deep-sea sediments. *Earth Planet. Sci. Lett.* **419,** 32–42 (2015).
32. Young, E. D., Galy, A. & Nagahara, H. Kinetic and equilibrium mass-dependent isotope fractionation laws in nature and their geochemical and cosmochemical significance. *Geochim. Cosmochim. Acta* **66,** 1095–1104 (2002).
33. Heuser, A. & Eisenhauer, A. The calcium isotope composition ($\delta^{44/40}$Ca) of NIST SRM 915b and NIST SRM 1486. *Geostand. Geoanal. Res.* **32,** 311–315 (2008).
34. Hippler, D. *et al*. Calcium isotopic composition of various reference materials and seawater. *Geostand. Newslett.* **27,** 13–19 (2003).
35. Jacobson, A. D., Andrews, M. G., Lehn, G. O. & Holmden, C. Silicate versus carbonate weathering in Iceland: new insights from Ca isotopes. *Earth Planet. Sci. Lett.* **416,** 132–142 (2015).
36. Risacher, F. & Clement, A. A computer program for the simulation of evaporation of natural waters to high concentration. *Comput. Geosci.* **27,** 191–201 (2001).
37. Hensley, T. M. *Calcium Isotopic Variation in Marine Evaporites and Carbonates: Applications to Late Miocene Mediterranean Brine Chemistry and Late Cenozoic Calcium Cycling in the Oceans* PhD thesis, Univ. California (2006).
38. Zeebe, R. E. & Wolf-Gladrow, D. A. *CO_2 in Seawater: Equilibrium, Kinetics, Isotopes* Vol. 65 (Elsevier Oceanography Series, 2001).
39. Fantle, M. S. & Higgins, J. The effects of diagenesis and dolomitization on Ca and Mg isotopes in marine platform carbonates: implications for the geochemical cycles of Ca and Mg. *Geochim. Cosmochim. Acta* **142,** 458–481 (2014).
40. Blake, T. S. Cyclic continental mafic tuff and flood basalt volcanism in the Late Archaean Nullagine and Mount Jope Supersequences in the eastern Pilbara, Western Australia. *Precambrian Res.* **107,** 139–177 (2001).
41. Lipple, S. Definitions of new and revised stratigraphic units of the eastern Pilbara region. *Annu. Rep.–West. Aust. Dep. Mines* **1974,** 98–103 (1975).
42. Bolhar, R. & Van Kranendonk, M. J. A non-marine depositional setting for the northern Fortescue Group, Pilbara Craton, inferred from trace element geochemistry of stromatolitic carbonates. *Precambrian Res.* **155,** 229–250 (2007).
43. Thorne, A. & Trendall, A. F. *Geology of the Fortescue Group, Pilbara Craton, Western Australia* Vol. 144 (Geological Survey of Western Australia, 2001).
44. Knoll, A. H. & Beukes, N. J. Introduction: initial investigations of a Neoarchean shelf margin-basin transition (Transvaal Supergroup, South Africa). *Precambrian Res.* **169,** 1–14 (2009).
45. Sumner, D. Y. & Beukes, N. J. Sequence stratigraphic development of the Neoarchean Transvaal carbonate platform, Kaapvaal Craton, South Africa. *South Afr. J. Geol.* **109,** 11–22 (2006).
46. Truswell, J. & Eriksson, K. Stromatolitic associations and their palaeo-environmental significance: a re-appraisal of a Lower Proterozoic locality from the northern Cape Province, South Africa. *Sediment. Geol.* **10,** 1–23 (1973).
47. Paris, G., Adkins, J., Sessions, A., Webb, S. & Fischer, W. Neoarchean carbonate-associated sulfate records positive Δ^{33}S anomalies. *Science* **346,** 739–741 (2014).
48. Sami, T. T. & James, N. P. Peritidal carbonate platform growth and cyclicity in an early Proterozoic foreland basin, Upper Pethei Group, northwest Canada. *J. Sediment. Res.* **64,** 111–131 (1994).
49. Sami, T. T. & James, N. P. Synsedimentary cements as Paleoproterozoic platform building blocks, Pethei Group, northwestern Canada. *J. Sediment. Res.* **66,** 209–222 (1996).
50. Hotinski, R. M. *Life's Influence on the Sedimentary Record: The Interplay of Ocean Chemistry, Circulation, and the Biological Pump* PhD thesis, Univ. Pennsylvania State (2000).